

This article was downloaded by:

On: 24 January 2011

Access details: *Access Details: Free Access*

Publisher *Taylor & Francis*

Informa Ltd Registered in England and Wales Registered Number: 1072954 Registered office: Mortimer House, 37-41 Mortimer Street, London W1T 3JH, UK



Journal of Macromolecular Science, Part A

Publication details, including instructions for authors and subscription information:

<http://www.informaworld.com/smpp/title~content=t713597274>

Microphase Structure of Oligoesteracrylate Networks Obtained by Anionic Polymerization in Various Solvents

V. V. Shilov^a; T. E. Lipatova^a; L. S. Kuzmenko^a; Ye. S. Shevchuk^a; V. A. Bogdanovich^a

^a Institute of Macromolecular Chemistry Ukrainian Academy of Sciences, Kiev, USSR

To cite this Article Shilov, V. V. , Lipatova, T. E. , Kuzmenko, L. S. , Shevchuk, Ye. S. and Bogdanovich, V. A.(1983) 'Microphase Structure of Oligoesteracrylate Networks Obtained by Anionic Polymerization in Various Solvents', Journal of Macromolecular Science, Part A, 20: 5, 627 – 653

To link to this Article: DOI: 10.1080/00222338308061797

URL: <http://dx.doi.org/10.1080/00222338308061797>

PLEASE SCROLL DOWN FOR ARTICLE

Full terms and conditions of use: <http://www.informaworld.com/terms-and-conditions-of-access.pdf>

This article may be used for research, teaching and private study purposes. Any substantial or systematic reproduction, re-distribution, re-selling, loan or sub-licensing, systematic supply or distribution in any form to anyone is expressly forbidden.

The publisher does not give any warranty express or implied or make any representation that the contents will be complete or accurate or up to date. The accuracy of any instructions, formulae and drug doses should be independently verified with primary sources. The publisher shall not be liable for any loss, actions, claims, proceedings, demand or costs or damages whatsoever or howsoever caused arising directly or indirectly in connection with or arising out of the use of this material.

Microphase Structure of Oligoesteracrylate Networks Obtained by Anionic Polymerization in Various Solvents

V. V. SHILOV, T. E. LIPATOVA, L. S. KUZMENKO,
YE. S. SHEVCHUK, and V. A. BOGDANOVICH

Institute of Macromolecular Chemistry
Ukrainian Academy of Sciences
Kiev 252160, USSR

ABSTRACT

The microheterogeneous structure of network polymers obtained from oligoesteracrylates of anionic polymerization has been studied. The parameters of microheterogeneity of these networks were calculated in the basis of wide- and small-angle x-ray diffraction. The causes of a very distinct microheterogeneity of oligoesteracrylate gels and a model of microphase structure of such gels were found within the scope of nonlinear thermodynamics of the irreversible processes.

The cross-linked polymers are, as a rule, microheterogeneous systems. Earlier, we made an attempt to determine the causes of the appearance of the heterogeneity. The cross-linked polyurethanes have been studied where the microheterogeneity exists even at the initial reaction stages due to strong intermolecular interaction and the presence of blocks of various chemical nature [1]. Later, depending on the relation between the flexible and rigid blocks in the process of reaction, the microheterogeneity was pronounced either more or less, being, however,

at the same level as the microheterogeneity of the initial system [2].

At present it is well known that when the formation of polymeric networks from oligoesteracrylates proceeds by the living anionic polymerization mechanism, the cross-linked polymers have developed a heterogenic structure [3-7] associated with the presence of microregions of various electron densities, these microregions being irregularly distributed throughout the polymer volume. In one of our earlier works dealing with the anionic polymerization of oligoesteracrylates (OEA) in a solution influenced by the sodium-naphthalin complex, we found that the network formation arises not from the microgel particles as in the case of the polyurethanes [8], but from large, highly branched, soluble molecules [9]. In this case micropores measuring several tens to hundreds of angstroms arise in the volume of the washed and dried polymer. Structural investigations show that the parameters of the microporous structure of the anionic networks of the OEA depend on such factors as the length of the initial oligomer molecule and the concentration of the solvent in the system being polymerized [5-7].

The present work was aimed at finding the causes of the appearance of the microheterogeneous structure of the cross-linked polymer which is formed from branched macromolecules carrying like charges. It seems natural that the heterogeneity of such systems is directly connected with the solvent-removal processes. However, there are no direct structural data which would allow one to ascertain the origin of the heterogeneity: either the processes of removing the solvent which is uniformly distributed throughout the volume of the initial swollen polymer, or the processes of network formation as a result of anionic three-dimensional polymerization, these processes leading to heterogeneity appearing in the initial gel. It would be equally desirable to ascertain the interrelation between the heterogeneity of swollen and dried polymer networks and the nature of the solvent used in polymerization.

SPECIMEN PREPARATION

To synthesize the polymers, α,ω -dimethacryl-bis(diethyleneglycol) phthalate (OEA-2) was used. This oligomer was purified by adsorption on chromatographic columns filled with activated aluminum oxide. The purification quality was controlled by the value of the refractive index which is 1.4998 for the OEA-2. The solvents (tetrahydrofuran, THF; toluene, T; hexane, H; methanol) were purified by known techniques [10]. The polymerization of OEA-2 was carried out by our usual technique [11]. Sodium naphthalene, prepared as described in Ref. 12, was used as the anionic polymerization catalyst. The synthesis was carried out in solutions of THF or in mixtures of THF-T and THF-H. The polymerization of OEA-2 in mixed solvents was carried out at a ratio of 1:1 of THF:T and at a ratio of 1:0.25 of THF:H.

The solvents for polymerization and the ratio of reaction mixture

components were selected from the following considerations. Earlier it was shown [13] that in mixed solvents like THF-T the anionic polymerization rate is lower than in pure THF. The selected ratio of 1:1 of THF-T ensures a considerable slowing down of the reaction and comparatively good homogeneity of the obtained polymer visually. The hexane is a poor solvent for the oligoesteracrylates. The polymerization of OEA-2 in the mixture THF-T with an equal ratio of solvents results in very rapid gel formation as a result of which it is impossible to obtain monolithic polymeric material. At the same time, with the ratio of THF-H in the reaction mixture being 1:0.25, gel formation appears to occur in the same way as when the mixture THF-T with a ratio of 1:1 is used as the solvent. For structural investigations, freshly prepared samples in equilibrium with the solvent were used, as well as dried samples with the solvent removed by the inclusion method and which were then dried in vacuum. As a result of such treatment, gel contraction took place under very mild conditions.

EXPERIMENT PROCEDURE

Structural investigations were carried out by wide- and small-angle roentgenography. The diffractometric curves in wide angles were obtained by means of diffractometer DRON-2.0 in the emission of a copper anode filtered by a nickel filter. A proportional detector BDP-2 was employed to record the scattering radiation. The diffractograms were taken in the automatic step-scanning mode of the detector. The diffraction curves obtained were reduced to equal intensities of the primary beam and equal values of the scattering volume by the usual technique [14].

The small-angle investigations were conducted on an automatic diffractometer fitted with a camera of the Kratki type [15]. Here copper anode emission monochromated by total internal reflection and nickel filter was used. A scintillation counter BDS-6 was used as an x-ray radiation detector. The diffractograms were obtained in the automatic step-scanning mode of the detector.

To obtain diffractograms of the swollen gels, the samples were placed in lamsan air-tight cells. These cells contained an excess of the solvent to maintain the equilibrium between a cross-linked polymer and solvent. Dry samples were investigated in the form of plates 1 mm thick.

To reduce the small-angle scattering data to the absolute scale, a standard Lupolene sample from the laboratory of Prof. Kratki* [16] was used. To calculate the heterogeneous structure parameters, the small-angle scattering curves were processed according to the FFSAXC 3†

*We express our gratitude to Prof O. Kratki for giving us the Lupolene sample and for its recalibration.

†We are grateful to Dr Vonk for granting us the use of the FFSAXC program.

program [17, 18]. Within the framework of this program, the initial small-angle diffractograms were statistically processed and corrected to the wide-angle scattering contribution [19]. The curve tails were approximated by polynomial $I(X) = U_1 \cdot X^{-3} + U_2 + U_3 \cdot X^k$ (U_1 , U_2 , and U_3 are constants; X is the distance between the initial beam position and the current detector position; and k is selected as an even whole number providing the best agreement with the experiment). The thickness of the interphase transition layer E was determined according to the Vonk algorithm [19]. The value $(S/V)/\phi(I - \phi)$ was also calculated, where ϕ is the volume part of heterogeneity regions and S/V is the specific internal surface of the heterogeneous system.

Correlation functions $\gamma(r)$ were calculated from the small-angle scattering curves obtained according to the technique based on the FFSAXS3 program by means of the Fourier-Bessel transformation. The distribution functions for the diameters of microregions in the approximation of their spherical shape and the corresponding averaging sizes were found by means of the subprogram DISTRIBUTION. On the basis of absolute values of the small-angle scattering intensity, the mean square values of the electron density fluctuation for the systems under investigation were found.

EXPERIMENTAL RESULTS

The x-ray wide-angle scattering curves for the initial oligomer and swollen cross-linked polymers prepared on its basis are shown in Fig. 1. The curve of the oligomer OEA-2 is characterized by one diffuse intensity maximum with the peak at 20.2° . During transition to the polymer gel a feebly marked shoulder corresponding to the angle interval from 13 to 15° appears on the left-hand slope of this maximum. To a lesser degree this shoulder is marked on the scattering curve of a gel obtained in pure THF and is practically absent on the intensity curves of all other gels. The intensity maximum on the diffractograms of swollen networks corresponds to 19.2° and is shifted toward the smaller angles compared with the maximum of the intensity curve of the initial oligomer.

Wide-angle diffractograms of dried polymer networks are given in Fig. 2. The intensity maximum peaks for these polymers correspond to angle intervals from 19.0 to 19.4° . The presence of the shoulder on the left-hand slope of the diffuse maximum can be noted on all the scattering curves of dried networks. The latter, as already pointed out, is characteristic of the initial oligomer diffraction curve. However, in contrast to the latter, the above shoulder is marked more distinct on the dry network diffractograms.

Figure 3 shows small-angle scattering curves of freshly polymerized gels. These curves are the result of the subtraction of the wide-angle scattering contributions from the primary diffraction data. It can be noted that all the above-mentioned curves are characterized by

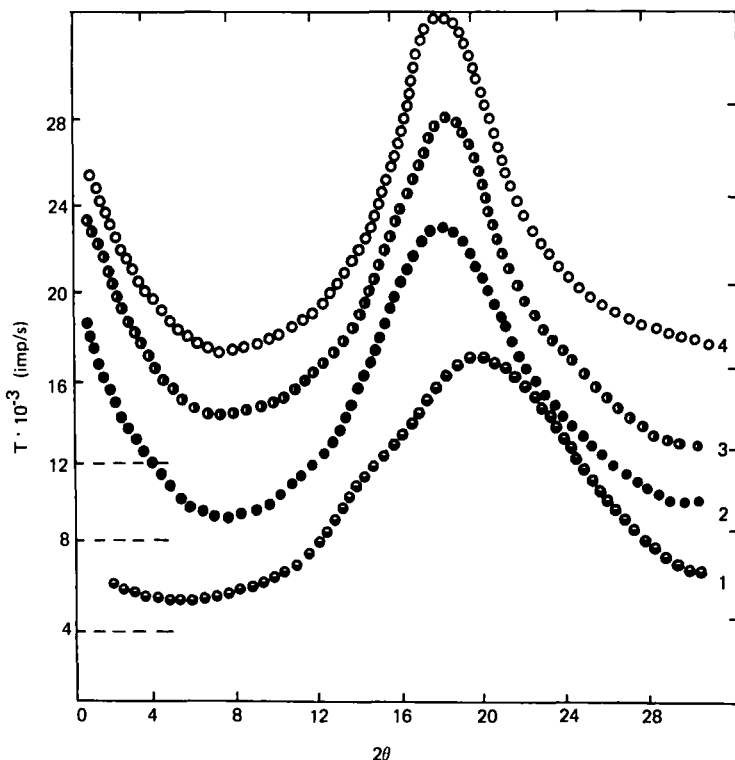


FIG. 1. Wide-angle x-ray scattering curves of gels: (1) initial oligomer; (2-4) polymers obtained in THF, THF-H, and THF-T, respectively.

a considerably higher absolute level than the corresponding small-angle scattering curves for typical one-component amorphous polymer materials [20-22]. A characteristic feature of the curves in Fig. 3 is the absence of any traces of interference maxima. A swollen network prepared in the mixture THF-T has the highest small-angle scattering level, while a network polymerized in pure THF has the lowest level. In the latter polymer an extremely slow drop of intensity can be noted with an increase of the scattering angle. Comparison of the small-angle scattering curves for various gels also permits it to be noted that in the cross-linked polymer obtained in the mixed solvent THF-H a more drastic drop of the intensity is manifested with an angle increase than in all other gels studied.

Small-angle scattering curves of the dried oligoesteracrylate network are given in Fig. 4. These curves were obtained by means of the

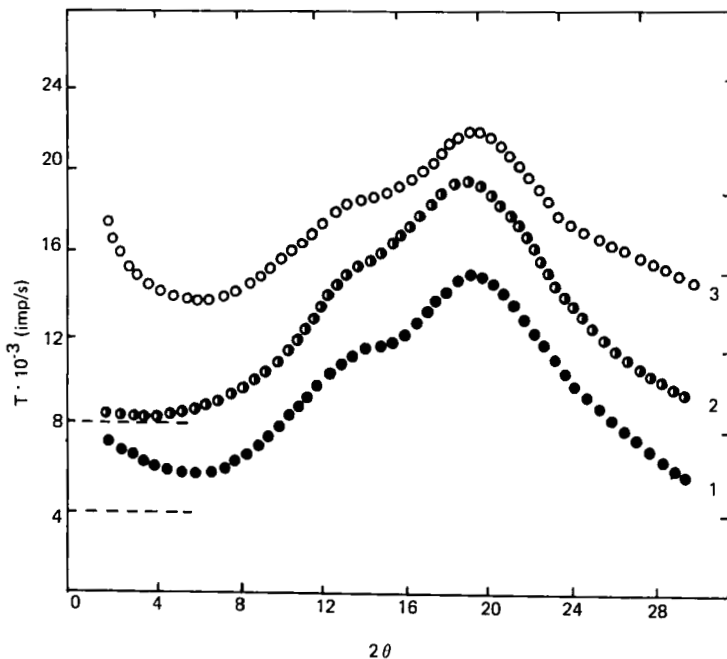


FIG. 2. Wide-angle x-ray scattering curves of dried polymers obtained in THF, THF-H, and THF-T (Curves 1, 2, and 3, respectively).

same treatment of diffraction data as the curves shown in Fig. 3. As can be seen, the small-angle scattering level for the dried networks decreases in the series of polymers prepared in the media THF-T, THF-H, THF. On the diffraction curve of the first polymer in these series a very smooth intensity drop with an increase of the scattering angle is observed. In this respect the scattering curve of this polymer differs considerably from the corresponding curves of all other dried gels. Comparison of curves shown in Figs. 3 and 4 makes it possible to note that the removal of the solvent results in the appearance of a more distinct angle dependence of the scattering intensity. At the tall part of the small-angle scattering curves for dried networks, the intensity is, as a rule, lower than in the curves for gels, whereas in the region of ultimately small angles the opposite is observed.

Figure 5 shows correlation curves for a network polymerized in THF medium. One of these curves refers to a swollen network, the other to a dry sample. It is evident that the removal of the solvent results in significant changes in the correlation curve of this sample.

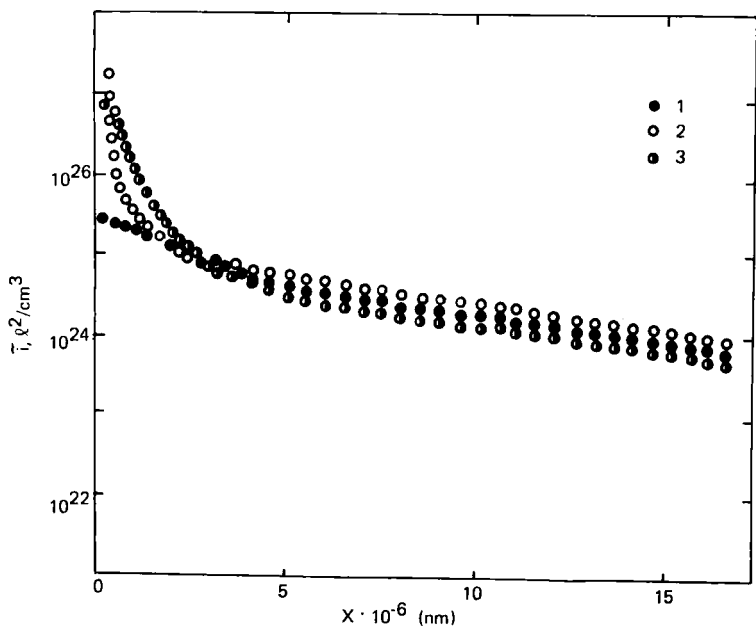


FIG. 3. Small-angle x-ray scattering curves of gels obtained in THF, THF-H, and THF-T (Curves 1, 2, and 3, respectively).

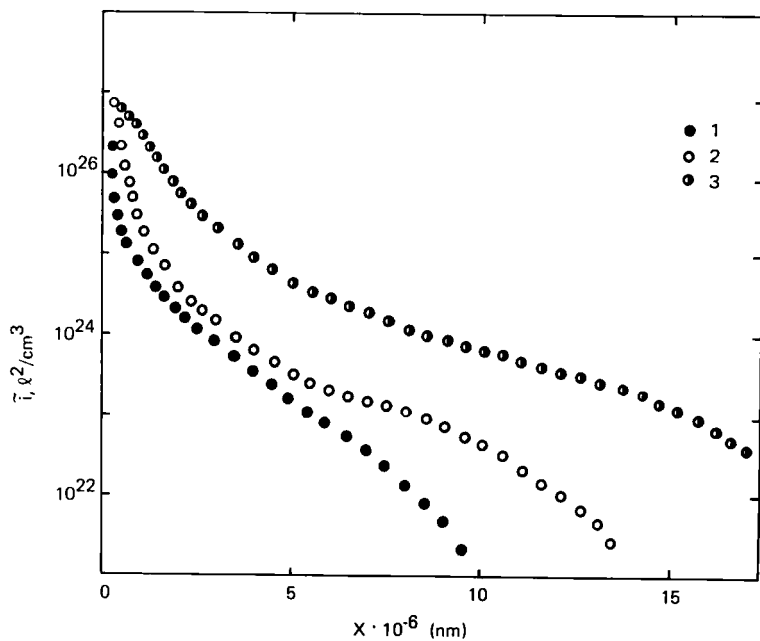


FIG. 4. Small-angle x-ray scattering curves of dried polymer networks obtained in THF, THF-H, and THF-T (Curves 1, 2, and 3, respectively).

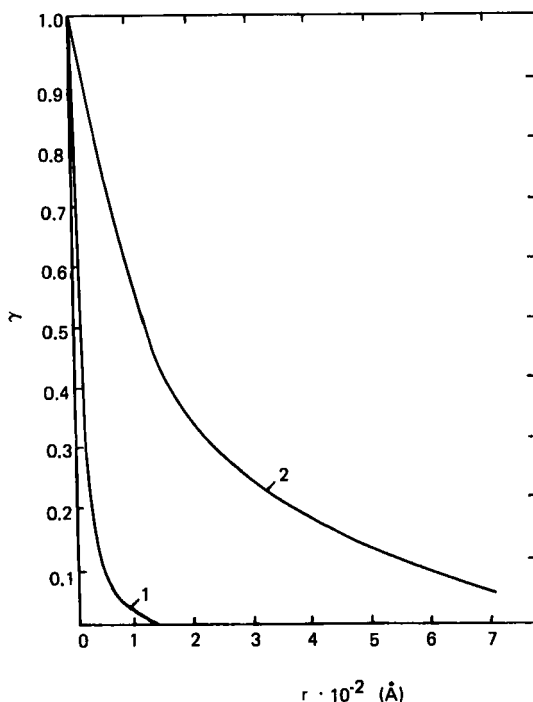


FIG. 5. Curves of correlation function $\gamma(r)$ for samples obtained in THF. Curve 1 refers to swollen sample, Curve 2 refers to dry sample.

In particular, it was shown that for the curve $\gamma(r)$ of a swollen network there is no noticeable contribution of distances greater than 100 \AA . At the same time, on this curve for a dry polymer a smooth drop is observed down to the distances of 800 \AA .

Figure 6 shows functions $\gamma(r)$ for swollen and dry networks prepared in the mixed solvent THF-H. The gel correlation function drops sharply in the region of radial distances down to 50 \AA . Then, up to 750 \AA , γ is characterized by a feebly marked dependence upon r . The correlation curve of a dry sample is similar to the corresponding curve of Fig. 5, but differs from the latter by a more even drop of γ with an increase of r .

Figure 7 shows the correlation curves $\gamma(r)$ for a gel and dry sample obtained in a medium of the mixed solvent THF-T. As can be seen, in this case the removal of the solvent from the network leads to extremely negligible changes in the $\gamma(r)$ /curve.

The absence of interparticle interference on small-angle scattering curves makes it possible to consider the corresponding functions

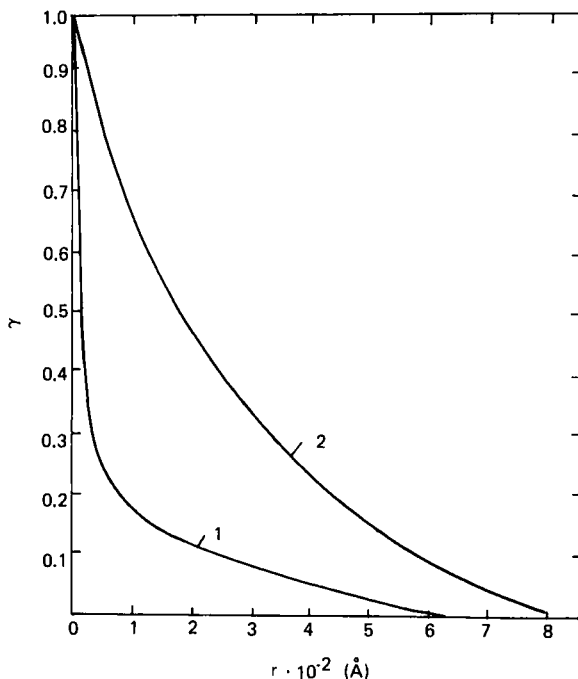


FIG. 6 Correlation curves of function $\gamma(r)$ for samples obtained in mixture THF-H. Curve 1 refers to swollen sample, Curve 2 refers to dry sample.

$\gamma(r)$ (Figs. 5-7) in the proximity of random distribution of the heterogeneity regions. As is well known [23], in such cases the function $\gamma(r)$ can be presented as a sum of weighed exponents

$$\exp(-r/l_p)$$

where r is the radial distance and l_p is the so-called correlation distance for this microregion.

Hence, by analyzing the dependence $\ln \gamma(r) = f(r)$, the preferential values of l_p can be determined by the tangent of its linear part.

Figure 8 illustrates the dependences $\ln \gamma(r) = f(r)$ for the gels studied, and Fig. 9 illustrates those for dry samples. Values of l_p found from these data are given in Table 1. As can be seen, for network prepared in THF solution, the swollen state is characterized by two parts of the dependence $\ln \gamma(r) = f(r)$ and, correspondingly, by two values of l_p . Both of them do not exceed several tens of angstroms.

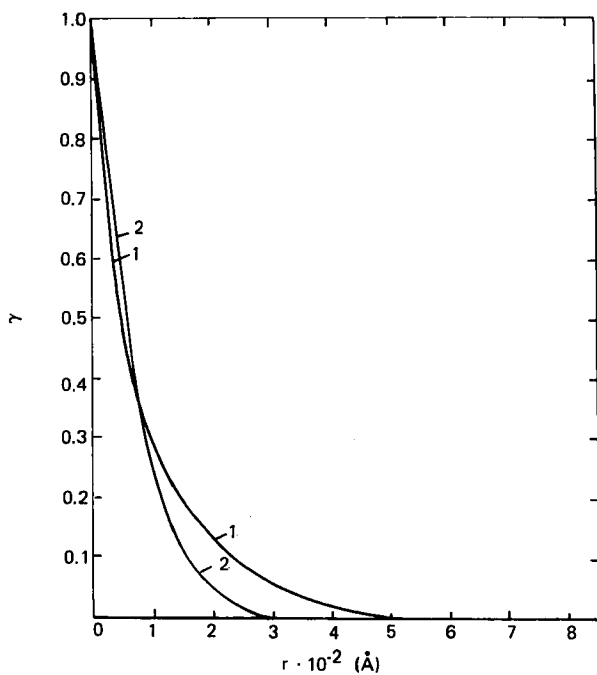


FIG. 7. Correlation curves of function $\gamma(r)$ for samples obtained in mixture THF-T. Curve 1 refers to swollen sample; Curve 2 refers to dry sample.

In the case of a swollen sample prepared in the mixed solvent THF-H, two linear parts of dependence sections $\ln \gamma(r) = f(r)$ are also present. One of them corresponds to l_p equal to 20 Å, the other being an order higher. With the removal of the solvent the specific salient point on the dependence $\ln \gamma(r) = f(r)$ disappears so that for the dry network we have l_p equal to 280 Å. Thus, large microregions of heterogeneous structure are present in a dry network.

As already observed, for a cross-linked polymer obtained in the mixed solvent THF-T there is observed a similarity of functions $\gamma(r)$ for a freshly prepared gel and a dry sample. The latter is reflected in similar values of l_p for dry and swollen polymers. Here, in the case of the gel, two linear parts similar in their inclination on the dependence $\ln \gamma(r) = f(r)$ can be distinguished. For a dry sample there is only one linear part on this dependence. However, the l_p value corresponding to this part is similar to l_p for the swollen network and,

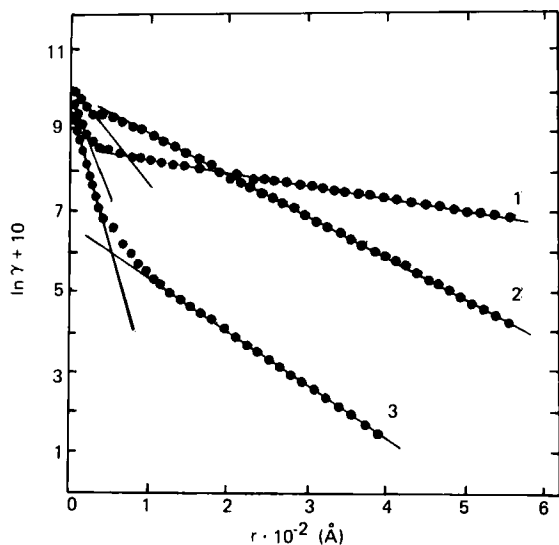


FIG. 8. Logarithmic dependence of function $\ln \gamma(r) = f(r)$ for swollen samples. Curves 1, 2, and 3 refer to polymers obtained in THF-H, THF, and THF-T, respectively.

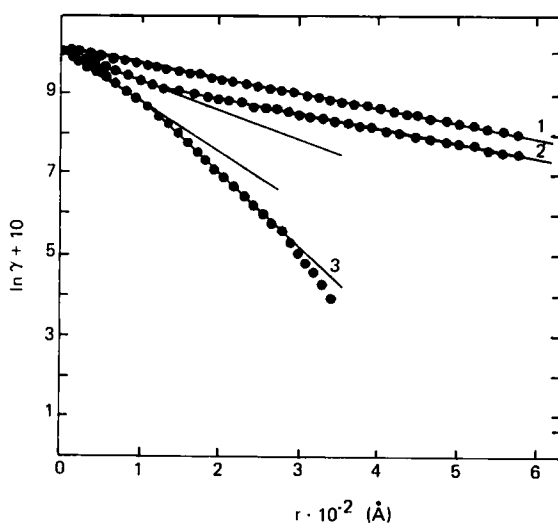


FIG. 9. Logarithmic dependence of function $\ln \gamma(r) = f(r)$ for dry samples. Curves 1, 2, and 3 refer to polymers obtained in THF-H, THF, and THF-T, respectively.

TABLE 1. Characteristics of Microheterogeneous Structure of Samples Obtained from OEA-2 at a Catalyst Concentration of 0.15 mol/L and a Ratio of Oligomer:Solvent of 1:1

Sample	$\left(\frac{\Delta \rho^2}{\text{mol}^2 \cdot \text{e}^2}\right)$ (cm^6)	l_p (\AA)	E (\AA)	$(S/V)/\phi$ ($1 - \phi$), cm^{-1}
No. 1. Swollen obtained in mixture THF-T = 1:1	1.55×10^{-3}	34	4.13	0.247×10^8
		112		
No. 2. Swollen obtained in mixture THF-H = 1:0.25	1.25×10^{-3}	20	5.30	0.516×10^8
		330		
No. 3. Swollen obtained in THF	0.745×10^{-3}	16	4.76	0.400×10^8
		83		
No. 4. Same as No. 1 dry	1.47×10^{-3}	70	3.52	0.482×10^7
No. 5. Same as No. 2 dry	0.197×10^{-3}	140	13.23	0.246×10^7
		275		
No. 6. Same as No. 3 dry	0.0064×10^{-3}	289	8.67	0.574×10^7

TABLE 1 (continued)

Sample	$\bar{\rho}$ $\left(\frac{\text{mol} \cdot e}{\text{cm}^3}\right)$	d (g/cm ³)	D_n (Å)	D_s (Å)	D_v (Å)	D_{guam} (Å)	$D_{\text{surf.}}$ (Å)	D_{volume} (Å)
No. 1. Swollen obtained in mixture THF-T = 1:1	-	-	13	23	150	38	63	193
No. 2. Swollen obtained in mixture THF-H = 1:0.25	-	-	12	12	40	42	40	70
No. 3. Swollen obtained in THF	-	-	13	16	44	40	40	46
No. 4. Same as No. 1 dry	0.643	1.212	23	127	200	62	126	197
No. 5. Same as No. 2 dry	0.628	1.180	19	133	299	112	188	303
No. 6. Same as No. 3 dry	0.643	1.209	14	75	217	74	134	229

eventually, is the average of these values. Thus the cross-linked polymer obtained in the THF-T mixture is characteristic of small microregions of heterogeneous structure.

Computer analysis of the small-angle scattering intensity functions, which permits determining the curves of the microregion distribution by size, has been performed in the approximation of the absence of correlation in the positions of separate microregions of heterogeneous structure [23].

The distribution curves of heterogeneous region diameters for freshly prepared gels and dry networks are given in Figs. 10 and 11. From these curves it is evident that the gels prepared in THF and THF-T are characteristic of comparatively narrow distributions of the heterogeneity microregions by size. During the transition to gel obtained in THF-H, the distribution function becomes asymmetrical and broadens toward large diameters. In dried cross-linked polymers a considerable asymmetry of functions $D_n(d)$ is observed: all of them have prolonged tails at the end of the large microregion diameters. The distribution curves of networks prepared in THF and THF-H acquire a bimodal shape, while in a network obtained in THF-T this effect is not observed.

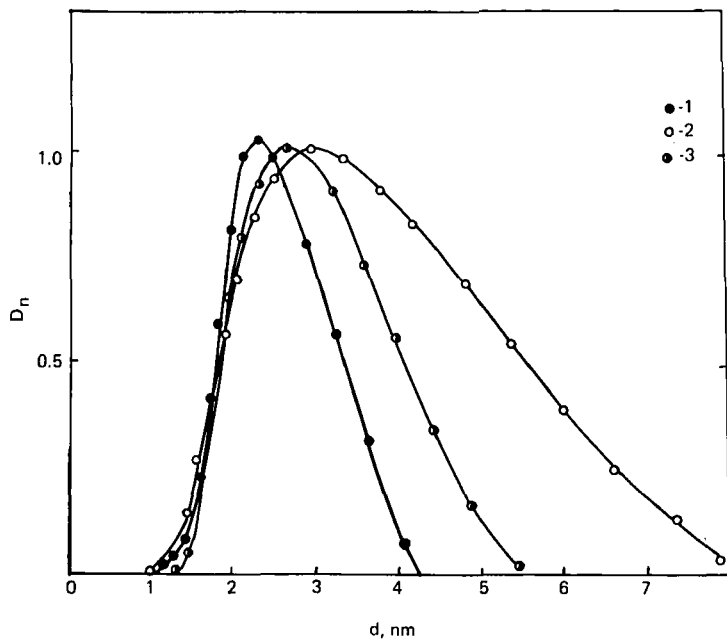


FIG. 10. Functions of heterogeneous microregion diameter distribution for gels obtained in THF, THF-H, and THF-T (Curves 1, 2, and 3, respectively).

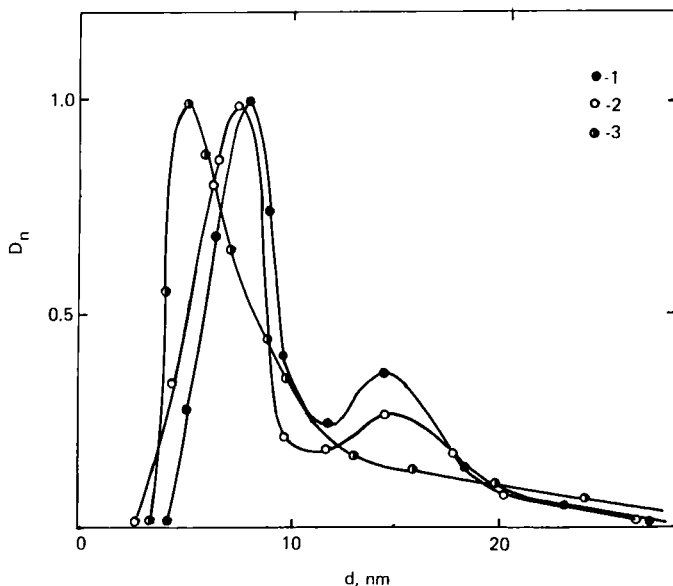


FIG. 11. Functions of heterogeneous microregion diameter distribution for dried polymers obtained in THF, THF-H, and THF-T (Curves 1, 2, and 3, respectively).

Figures 12 and 13 show experimental small-angle scattering curves of the systems studied in comparison to the theoretical curves obtained by means of a reverse calculation of the microregion diameters distribution functions (Figs. 10 and 11) into the intensity functions. Satisfactory agreement of experimental and calculated data is noted. This signifies the reliability of the calculated distribution functions. Comparing the specific features of these curves with the l_p values for the microheterogeneous structure obtained by both methods are in agreement. Here, it must be noted that the analysis of dependences $\ln \gamma(r) = f(r)$ yields dimensional characteristics of the heterogeneous structure without taking into account the relative fraction of various microregions. At the same time, the by-size-distribution curves offer, within the scope of the above-mentioned approximations (sphericity and random microregion disposition), an absolutely strict estimate of the fraction of the regions having this or that diameter. As can be seen from Figs. 10 and 11, the amount of comparatively large microregions (of the order of hundreds of angstrom) is relatively small in all the systems under investigation. This is also supported by the values of size characteristics given in Table 1 which were obtained by averaging the num-

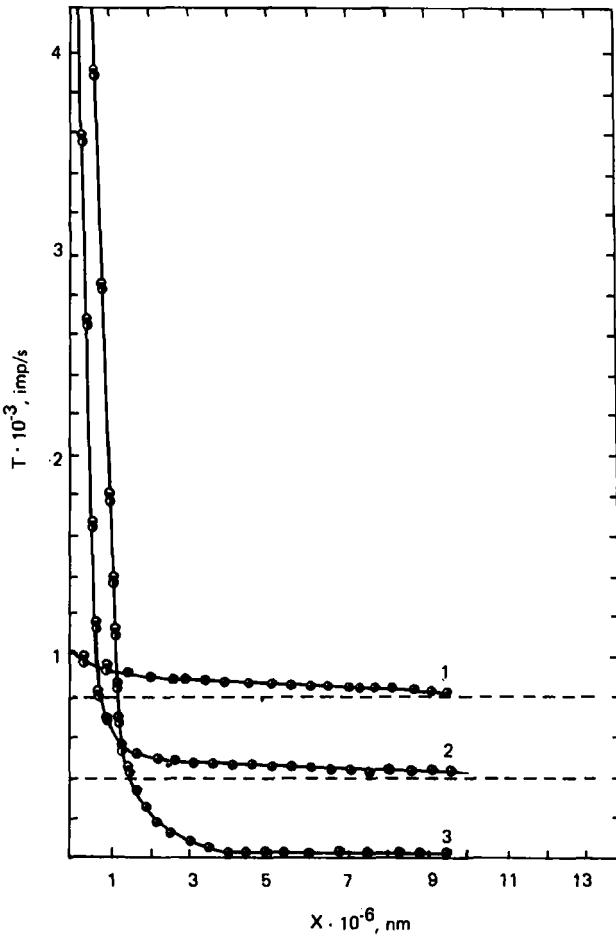


FIG. 12. Experimental small-angle scattering curves of swollen samples and theoretical curves obtained by distribution function inverse recalculation. Curves 1, 2, and 3 refer to samples obtained in THF, THF-H, and THF-T, respectively.

ber of microregions (D_n), their surface (D_s), and their volumes (D_v) by their functions throughout the entire range of diameters (from 0 to 800 Å). As is evident, the number-average characteristics are within the range of 10 to 20 Å. A more or less distinct excess of D_s and D_v values over D_n can be observed. The degree of these excesses rises with the increase of the microregion polydispersities.

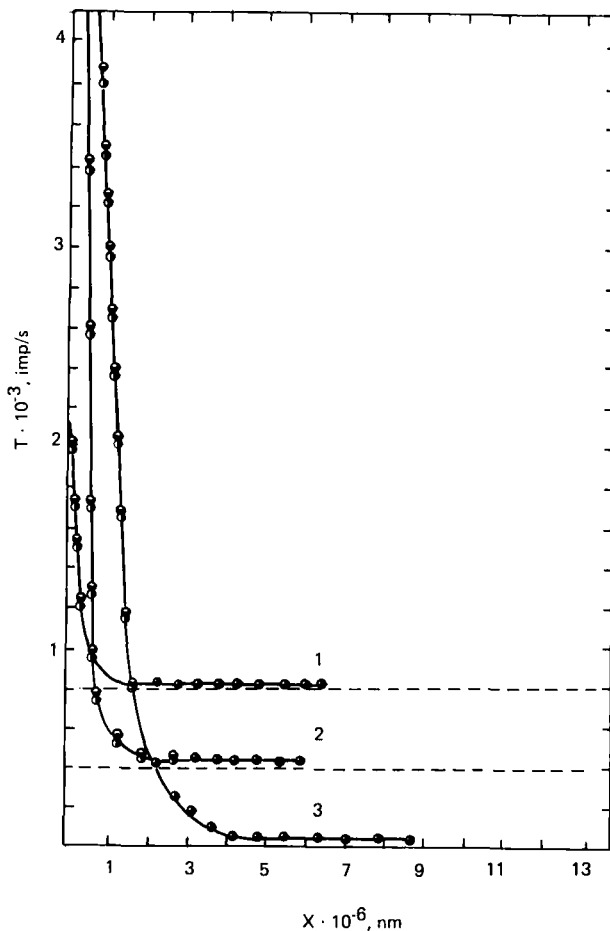


FIG. 13. Experimental and theoretical small-angle scattering curves of dried samples obtained by inverse recalculation of the distribution function. Curves 1, 2, and 3 refer to samples obtained in THF, THF-H, and THF-T, respectively.

The thickness of the interphase transition layer E also belongs to the size characteristics of the microheterogeneous structure. The respective values of E for the investigated gels and dry networks are given in Table 1. The table shows that the systems studied are characteristic of comparatively small values of E (from 4 to 13 Å). So, in swollen and dried networks prepared in the mixed solvent THF-T, the interphase layer thicknesses are quite close (4 Å). In a dry net-

work prepared in THF, the E value is twice that of a gel (8 and 4 Å, respectively). Solvent removal from a network prepared in the mixture THF-H also leads to an increase of the transition layer thickness.

As is well known, the specific surface (S/V) is one of the most significant characteristics of heterogeneous systems. It does not seem possible to determine the absolute values of S/V within the scope of calculations carried out, since there are no independent data on the volume fraction of the heterogeneity microregions. Therefore, we have found the values $(S/V)/\phi(1 - \phi)$ dependent both on the specific surface and on the volume fraction of one of the phases (data given in Table 1). In the gel series, as well as in the series of dried networks, these characteristics change within small limits. However, in the case of dry networks values, $(S/V)/\phi(1 - \phi)$ are one order smaller than those for the gels.

Table 1 gives also mean square values of electron density fluctuation, these values directly reflecting the contrast of the heterogeneous structure of the investigated cross-linked polymers. Comparison of these values shows great differences in $\Delta\rho^{-2'}$ (from 0.64×10^{-5} to $1.55 \times 10^{-3} \text{ e}^2 \cdot \text{mol}^2 / \text{cm}^6$). The removal of the solvent from freshly prepared gels obtained in pure THF leads to a decrease of $\Delta\rho^{-2'}$ by two orders. In the case of a network prepared in the THF-H mixture, a similar change of $\Delta\rho^{-2'}$ is observed. Only polymerization in the mixed solvent THF-T produces gel whose mean square of electron density fluctuation is almost the same as in a dry sample.

It can be noted that in freshly prepared gels obtained in THF-T, THF-H, and THF, about a twofold reduction of $\Delta\rho^{-2'}$ is observed. The values of $\Delta\rho^{-2'}$ decrease in the same succession in dry networks as well, but in them the differences in $\Delta\rho^{-2'}$ in the indicated series are more significant (being over two orders).

DISCUSSION

The data on wide-angle x-ray scattering by the systems studied permits us to assert the absence of long-range order in the arrangement of adjacent fractions of macromolecules both in networks in equilibrium with the solvent and in dry samples. By comparing the diffraction curves of Figs. 1 and 2 we can see that the short-range order in dry and swollen networks does not differ qualitatively from the short-range order in the oligomer liquid. Thus, the short-range order can be presented as a greatly distorted liquid-type lattice [24] formed by fractions of adjacent molecular chains.

One peculiarity of wide-angle diffractograms of the systems studied, associated with the appearance of a shoulder on the left-hand slope of

the main maximum, deserves attention. In the initial oligomer, in particular, the latter can be considered to result from essential differences in the packing of molecular chain fragments of the OEA-2 from their symmetrical (quasi-hexagonal) arrangement in the basal plane of the paracrystal lattice of a liquid oligomer. As is well known, this is typical of liquid polymers and oligomers with bulk substitutes in the main chain [25]. Thus, the appearance of the shoulder on the left-hand slope in the main maximum of the intensity curve for liquid oligomer can be considered as a characteristic feature of this compound, the feature being associated with the asymmetrical nature of its chain. A similar effect was noted by us in liquid oligopropylene glycol [26], which is also characterized by the presence of bulk side chains in the molecular chain.

The appearance of the characteristic shoulder on the left-hand slope of the main maximum of the wide-angle scattering curves for dry networks is the result of similar packing of the molecular chain fragments of the oligomer and the cross-linked polymers. At the same time, the differences in the wide-angle scattering curve profile observed in these samples signify that the replacement of solvent determined the differences in the short-range order in the cross-linked polymers of a practically identical chemical nature. In addition to that, inclusion of solvent molecules between the cross-linked polymer chains leads to a more symmetrical packing of molecule fragments in the basal plane of a corresponding paracrystal lattice.

The small-angle scattering data confirm the conclusion [6] about the high degree of structure heterogeneity of oligoesteracrylate networks obtained by anionic polymerization. The results of this study permit the additional conclusion to be drawn that the stated heterogeneity develops to a greater or lesser degree, depending on the solvent used in polymerization. It seems especially important that this work shows for the first time that the heterogeneity of oligoesteracrylate networks is displayed in a freshly-prepared polymer gel. Thus, this heterogeneity is the result of a nonuniform component distribution in the system oligomer-cross-linked polymer-solvent found after polymerization in the form of microregions of various electron densities.

Let us dwell more minutely on the analysis of the corresponding qualitative characteristics of these microregions. In the molecular size scale, the microregions measuring about 20 Å correspond to a volume containing some 20-25 molecular chains across the cross-section which, in our case, is approximately equal to the same quantity of OEA-2 molecules. In the cross-section of microregions measuring 100 Å, up to 400-600 fragments of OEA-2 can be packed, while in microregions measuring ~300 Å, about 10^4 similar fragments can be included. Accordingly, the heterogeneous-structure microregions distributed at random within the volume of swollen networks prepared in THF and THF-T may contain several tens of oligoesteracrylate networks chains whereas the microregions of a gel prepared in the mixed

solvent THF-H can contain several hundreds of such chains. Similar amount of chains can be packed into the cross-section of heterogeneous microregions of dried polymer prepared in THF-T. In contrast to this, dry networks prepared in THF-H and THF contain regions of local heterogeneity, the cross-sections of which could contain thousands of cross-linked molecular chains.

Upon examining the transition layer thicknesses found in this study on the molecular size scale, it can be noted that the minimum thickness corresponds to a cross-section of one chain, and the maximum thickness to that of three chains.

It is expedient to consider the mean-square values of electron density fluctuation given in Table 1 by comparing them with the theoretical estimations of this value of $\Delta \bar{\rho}_c^{-2}$. As is well known, $\Delta \bar{\rho}_c^{-2}$ can be calculated for a certain model of heterogeneous structure when the electron densities of the corresponding microregions (ρ_1 and ρ_2) and the volume fraction of the microregions of one of the phases (ϕ) are known:

$$\Delta \bar{\rho}_c^{-2} = \phi(1 - \phi)(\rho_1 - \rho_2)^2 \quad (1)$$

The values of electron densities of solvents used in the synthesis (THF, THF-H, and THF-T) are 0.494, 0.472, and 0.483 e·mol/cm³, respectively. Since the structure heterogeneity of the investigated gels has to be connected with the presence in their volume of microregions more or less enriched by solvent, then, using the above values of electron densities of components, the corresponding values of $\Delta \bar{\rho}_c^{-2}$ can be calculated for various heterogeneous structure models.

To obtain the estimates of $\Delta \bar{\rho}_c^{-2}$, we selected several of the simplest models of heterogeneous structure of oligoesteracrylate gels. In particular, in analyzing the first model, we proceeded from the point that the gel consists of pure solvent microregions distributed at random in the polymer matrix. It was also assumed that the content of components changes in the same way, this being close to reality. For the second model it was also assumed that the microregions of pure solvent are distributed at random in the polymer matrix. However, in this case the value was considered not to be fixed and was determined from relation (1) on the basis of condition $\Delta \bar{\rho}_c^{-2} = \Delta \bar{\rho}_c^{-2'}$. Thus, for systems with complete phase separation, the value of $\Delta \bar{\rho}_c^{-2}$ can be obtained from the first model at a definite value of ϕ , and from the second model a value of ϕ at $\Delta \bar{\rho}_c^{-2}$ is calculated which corresponds to the experimental mean square value of the electron density fluctuation. It should be noted that both models represent an ultimate case of microphase separation which in reality might not be realized. Yet,

it is possible to obtain useful information on the heterogeneous structure of real systems on the basis of estimates of $\Delta \bar{\rho}_c^{-2}$ and ϕ obtained for these models. Values of $\Delta \bar{\rho}_c^{-2}$ for the first model and those of ϕ for the second model are given in Table 2. It should be pointed out that $\Delta \bar{\rho}_c^{-2}$ for the first model exceeds by manyfold the values of $\Delta \bar{\rho}^{-2}$ found experimentally. Consequently, this model considerably overestimates the degree of microphase separation of components. The volume fractions of pure solvent in the second model do not exceed 6%. At the same time, according to preliminary estimates, the gels studied contain not less than 40% of solvent. Thus it follows that the second model does not take into account all the solvent contained in the gels studied. The fact that the microphase separation in a cross-linked polymer-solvent system does not take place at the level of pure components was taken into account in the third of the models which we analyzed. In particular, the calculations were carried out for a case where the matrix consists of 75% of a polymer and 25% of adducts, the polymer:solvent ratio in the system being 1:1. Values of $\Delta \bar{\rho}_c^{-2}$ obtained in these calculations are given in Table 2. It can be noted that for this model these values of $\Delta \bar{\rho}_c^{-2}$ prove to be close to the values of $\Delta \bar{\rho}^{-2}$. Especially satisfactory compliance is observed in the gel obtained in the mixed solvent THF-T. However, the trend in the change of values of $\Delta \bar{\rho}_c^{-2}$ in the series of gels obtained in THF-T, THF-H, and THF does not agree with the experimentally observed changes of $\Delta \bar{\rho}^{-2}$. The latter is evidently the result of the fact that this model of the heterogeneous-structure oligoesteracrylate gels cannot serve as an adequate approximation to reality from the quantitative point of view. It seems quite natural that the polymer-to-solvent ratio in the heterogeneous microregions, as well as the volume fraction of these microregions, varies in the transition from one gel studied to another. However, this is not accounted for in the results of calculation given in Table 2. Nevertheless, it should be pointed out that the last of the analyzed heterogeneous structure models of oligoesteracrylate gels, in a qualitative respect, correctly reflect the peculiarities of the structures of these systems.

Proceeding to the analysis of the value of $\Delta \bar{\rho}^{-2}$ for dry networks, it should be noted that changes of the mean-square electron density fluctuation upon solvent removal cannot be explained by assuming a symbatic changes of matrix volume and the heterogeneous regions distributed in it. In the first place, in this case a considerable contrasting of the heterogeneous structure should be expected as a result of the great density deficit in regions heretofore enriched by solvent. Actually, this has not been observed in any of the systems investigated. In the second place, a symbatic change of the microregion volumes of the

TABLE 2. Calculated Parameter Values of Heterogeneous Structure of Swollen Networks Obtained from OEA-2 in Various Solvents

Solvent	Model 1		Model 2		Model 3	
	ϕ	$\bar{\rho}_c \times 10^3$ $\left(\frac{\text{mol}^2 \cdot e^2}{\text{cm}^6}\right)$	ϕ	$\bar{\rho}_c \times 10^3$ $\left(\frac{\text{mol}^2 \cdot e^2}{\text{cm}^6}\right)$	ϕ	$\bar{\rho}_c \times 10^3$ $\left(\frac{\text{mol}^2 \cdot e^2}{\text{cm}^6}\right)$
THF	0.5	5.6	0.04	0.745	0.5	1.6
THF-H	0.5	7.2	0.05	1.25	0.5	1.7
THF-T	0.5	6.4	0.06	1.55	0.5	1.4

heterogeneous structure would be contradictory to the above data on the increase of the size of heterogeneity microregions in dry networks as compared to that of swollen ones. Thus, a solely logical interpretation of the microheterogeneous structure parameters observed upon solvent removal can consist in that that process is accompanied by structure rearrangement in the case of a network synthesized in a THF-T solution. Similar changes in the heterogenic structure can be considered comparatively small. However, in a network prepared in THF they lead actually to a complete disappearance of any traces of the heterogeneous structure in the initial gel.

A nonuniform solvent distribution in the initial gel volume is one of the most interesting and important features of the systems investigated. It seems natural that here a question arises about the causes of such vividly marked heterogeneity of swollen networks. In the polyurethane systems this was attributed to the formation of supermolecular structures like macromolecular aggregates in the initial oligomers [27]. The appearance of such aggregates in the solutions of OEA is unlikely. It is evidently impossible to find an explanation for the heterogeneity observed in the gels within the framework of the existence of the equilibrium supermolecular structures. Thus, it follows that this phenomenon should be attributed to the peculiarities of chemical reactions and diffusion processes in the system being polymerized.

Let us analyze to what degree the heterogeneity of the oligoesteracrylate networks can be related to the preceding chemical reactions and diffusion processes.

According to the formalism of the thermodynamics of irreversible processes [28], the peculiarities of such types of systems may be connected with the changes in the generalized flows (J_k) and corresponding generalized forces (X_k). The diffuse motive force for component j (X_j^{diff}) is determined by the relation

$$X_j^{\text{diff}} = - \Delta \frac{\mu_j}{T}$$

where $\Delta \mu_j$ is the chemical potential gradient for component J . The reaction motive force ρ (X_ρ^{react}) is determined on the basis of the expression

$$X_\rho^{\text{react}} = A_\rho / T$$

where $A = - \sum_j \mu_j \nu_{j\rho}$ is the reaction affinity and $\nu_{j\rho}$ is the stoichiometric coefficient for component j in reaction ρ .

In the case of ρ_j being the partial density of component j , then the variables describing the state of the system satisfy the following equilibrium equation.

$$\frac{\partial \rho_j}{\partial t} = -\text{div } \bar{J}_j + \sum_j \nu_{j\rho} \omega_\rho$$

where \bar{J}_j is the diffusion flow component j (a quantity of this component transferred into a time unit through a unit of surface limiting the separated volume), and ω_ρ is the reaction rate ρ per volume unit.

Any stationary process involves time changes of the entropy. Here the time-dependent entropy change due to internal processes in the system is defined as entropy production (P). In the region of linear thermodynamics of irreversible processes, when the flows are linear functions of forces, minimum entropy production takes place. In this case a homogeneous component distribution in the system is sustained [29]. If the deviation from the standard stationary state be expressed as corresponding entropy gains (ΔS) and entropy production (ΔP), we get the following relations:

$$\Delta S = S(\{\rho_j\}) - S^\circ(\{\rho_j\}) = \delta S + \frac{1}{2} \delta^2 S + \dots$$

$$\Delta P = \int dV \sum_k J_k X_k - \int dV \sum_k J_k^\circ X_k^\circ = \delta P + \frac{1}{2} \delta^2 P + \dots$$

(here the superscript denotes the stationary state).

The quadratic forms of $\delta^2 S$ and $\delta^2 P$ in the expansion of ΔS and ΔP values are decisive for the system behavior in the nonlinear region. The first form is a negatively determined value throughout the entire region of the application of local thermodynamics. The second form is a doubled value of the so-called excessive entropy production ($\delta_x P$). These values are bound by the following relation:

$$\delta_x P = \frac{d}{dt} \cdot \frac{1}{2} (\delta^2 S) = \int dV \sum_k \delta J_k \cdot \delta X_k$$

where δX_k and δJ_k are the variations of thermodynamic forces and currents.

Thus, from the above relations it follows that the stationary state becomes unsteady as soon as the excessive entropy production turns into a negative value. In this case the homogeneity of component distribution is upset and a steady-state is established which is characterized by the presence of some ordering, or, which is the same thing, by a nonuniform component distribution. The new steady-state mode is characterized by the appearance of dissipative structures reflecting such irregularity.

Since the thermodynamics of chemical reactions is in its essence the nonlinear thermodynamics of irreversible processes, the appear-

ance of heterogeneity in reacting systems is rather the rule than the exception. In instances where the diffusion flows are directed against the concentration gradient, the diffusion smooths out the local heterogeneity caused by the reaction proceedings. However, if the system, as a result of polymerization, proves to be inside the spinodal on a phase diagram, i.e., becomes unstable, the diffusion flows change their direction [29] and are unable to smooth the local heterogeneities. In this case the formation of the microheterogeneous state is a direct result of a so-called spinodal decomposition. In many cases the latter accompanies the polymerization processes in multicomponent systems [30].

Should we analyze the specific features of phase distribution according to the spinodal mechanism, it becomes evident that they are identical to a considerable degree with the processes of dissipative structure formation under conditions removed from equilibrium [30]. At the early stages of spinodal decomposition the system appears as a periodic alternation of microregions with slight deviations from the average composition. The sizes of such modulated structures attain tens and hundreds of angstroms [31, 32]. At later decomposition stages the microregions approach the equilibrium phases to a greater degree in their composition; they become larger when their specific periodicity arrangement is upset [33]. By analyzing the pattern of the microheterogeneous structure of the oligoesteracrylate gels formed by the anionic mechanism, a reasonable analogy suggests itself with the above peculiarities of systems undergoing phase separation in the unstable regions. The investigated gels exhibit microphase regions of the same order of the value with unresolved separation into polymer and solvent.

Thus, the above considerations permit a consistent explanation of the heterogeneous component distribution arising in the gels being studied. Since the interaction parameters of various solvent and oligoesteracrylate lattice differ, the conditions of heterogeneous structure formation in the corresponding gels also vary. This determines the peculiarities observed in the heterogeneous structure of gels prepared in THF, THF-H, and THF-T.

Additional peculiarities of the systems studied are determined by the equilibrium electric charge distribution in the gels even after termination of the polymerization process. Upon removal of these charges the swollen gels prove to be in a state even further removed from equilibrium than the system immediately after the termination of anionic polymerization. The nonequilibrium in the swollen anionic networks is the subject of future studies.

It seems that changes in the heterogeneous structure of the oligoesteracrylate networks, upon solvent removal, are, to a great extent, connected with the subsequent processes of phase separation due to the changing component ratio. Of course, they are also determined by the nature of the solvent used in polymerization. This is the basis for comprehending those great differences of the heterogeneous structure of dry networks obtained in various solvents.

REFERENCES

- [1] T. E. Lipatova, Catalytic Polymerization of Oligomers and Polymeric Network Formation, Naukova Dumka, Kiev, 1974 (in Russian).
- [2] V. V. Shilov and T. E. Lipatova, Vysokomol. Soed., **A**, 20, 62 (1978).
- [3] T. E. Lipatova, L. S. Kuzmenko, V. V. Shilov, and N. N. Minenko, Ibid., **20**, 2013 (1978).
- [4] V. V. Shilov, T. E. Lipatova, N. N. Minenko, and V. Knige, Sintez i splavy, Naukova Dumka, Kiev, 1978 (in Russian).
- [5] T. E. Lipatova, L. S. Kuzmenko, V. V. Shilov, and V. A. Bogdanovich, Kompositionnye polimernye materialy, Naukova Dumka, Kiev, 1980, p. 26 (in Russian).
- [6] T. E. Lipatova, L. S. Kuzmenko, and V. V. Shilov, J. Macromol. Sci.-Chem., **A13**(6), 777 (1979).
- [7] T. E. Lipatova, Ye. S. Shevchuk, V. V. Shilov, and V. A. Bogdanovich, Vysokomol. Soed., **A23**, 73 (1981).
- [8] A. E. Nesterov, T. E. Lipatova, V. K. Ivaschenko, and Yu. S. Lipatov, Ibid., **B12**, 150 (1970).
- [9] T. E. Lipatova, G. S. Shapoval, Ye. S. Shevchuk, and N. P. Basylevskaya, Ibid., **A14**, 2610 (1972).
- [10] T. E. Lipatova, G. S. Shapoval, Ye. S. Shevchuk, and N. P. Basylevskaya, Ibid., **A11**, 2280 (1969).
- [11] T. E. Lipatova, G. S. Shapoval, Ye. S. Shevchuk, and N. P. Basylevskaya, J. Macromol. Sci.-Chem., **A5**(2), 345 (1975).
- [12] T. E. Lipatova, G. S. Shapoval, Ye. S. Shevchuk, N. P. Basylevskaya, and T. I. Novikova, Sintez i Fisiko-Chimiya Polimerov, Vol. 15, Naukova Dumka, Kiev, 1975, p. 21 (in Russian).
- [13] Yu. S. Lipatov, V. V. Shilov, N. N. Minenko, and V. Knige, Fisiko-chimicheskiye svoystva i struktura polimerov, Naukova Dumka, Kiev, 1977 (in Russian).
- [14] T. E. Lipatova, V. V. Shilov, N. P. Basylevskaya, and Yu. S. Lipatov, Br. Polym. J., **9**(2), 159 (1976).
- [15] O. Kratky, I. Pilz, and P. I. Schmidt, J. Colloid Interface Sci., **21**(1), 24 (1966).
- [16] I. Pilz and O. Kratky, Ibid., **24**, 211 (1967).
- [17] C. G. Fonk, Program for the Processing of Small Angle X-Ray Scattering Data, FFSAXS, Geelen, Netherlands, 1975.
- [18] C. G. Fonk, Program for the Processing of Small Angle X-Ray Scattering Data, FFSAXS-3, Geelen, Netherlands, 1977.
- [19] C. G. Fonk, J. Appl. Crystallogr., **6**, 81 (1973).
- [20] J. H. Wendorf and E. V. Fischer, Kolloid-Z. Z. Polym., **251**, 884 (1973).
- [21] V. V. Shilov, N. N. Minenko, T. E. Lipatova, and Yu. S. Lipatov, Dokl. Akad. Nauk SSSR, **230**, 1162 (1976).
- [22] J. Rathie and W. Ruland, Colloid Polym. Sci., **251**, 358 (1976).

- [23] A. Guinier and G. Fournet, Small-Angle Scattering of X-Rays, Wiley, New York, 1955, p. 19.
- [24] R. Hosemann, G. Willmann, and R. Rolsler, Phys. Rev.: Gen. Phys., **6**, 2243 (1972).
- [25] H. G. Kilian and K. Boueke, J. Polym. Sci., **58**, 311 (1962).
- [26] Yu. S. Lipatov, V. V. Schilov, Yu. P. Gomza, and N. E. Kruglyak, Rentgenograficheskie metody izycheniya polimernykh sistem, Naukova Dumka, Kiev, 1982, p. 234 (in Russian).
- [27] T. E. Lipatova, Cataliticheskaya polymerizatsiya oligomerov i formirovanie polimernykh setok, Naukova Dumka, Kiev, 1974, (in Russian).
- [28] P. Glansdorff and I. Prigogine, Thermodynamic Theory of Structure, Stability and Fluctuations, Wiley, London, 1971.
- [29] G. Nikolis and I. Prigogine, Self-Organization in Nonequilibrium Systems, Wiley, New York, 1977.
- [30] P. H. Lindenmeyer, Polym. J., **11**, 677 (1979).
- [31] G. W. Cahn and J. E. Hilliard, J. Chem. Phys., **31**, 688 (1959).
- [32] J. W. Cahn, Acta Metall., **11**, 1245 (1963).
- [33] J. W. Cahn, Ibid., **42**, 93 (1965).

Accepted by editor February 28, 1983

Received for publication March 30, 1983